



北京理工大学
BEIJING INSTITUTE OF TECHNOLOGY



Fully Automated Left Atrial Segmentation from MR Sequences Using Deep Convolutional Neural Network and Unscented Kalman Filter

Xiaoran Zhang^{1,2,3*}, Glynn Martin^{1,2}, Michelle Noga^{1,2}, Kumaradevan Punithakumar^{1,2,4}

¹ Department of Radiology and Diagnostic Imaging, University of Alberta, Edmonton, Canada

² Servier Virtual Cardiac Centre, Mazankowski Alberta Heart Institute, Edmonton, Canada

³ School of Automation, Beijing Institute of Technology, Beijing, China

⁴ Department of Computing Science, University of Alberta, Edmonton, Canada

* Corresponding Author

Outline

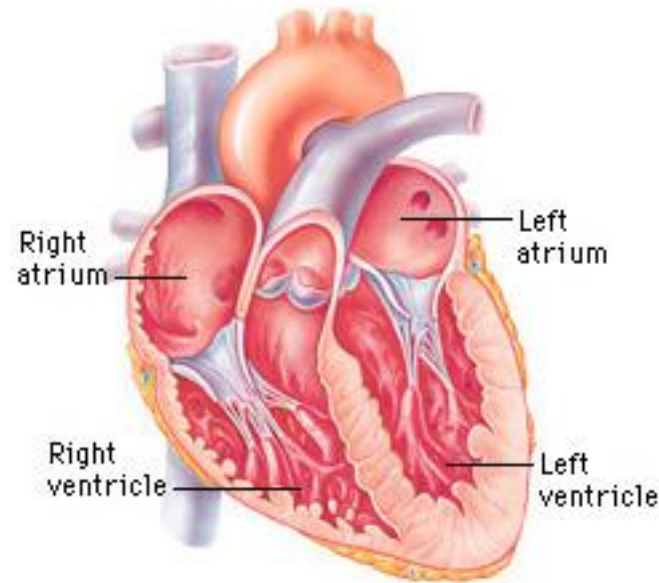
- Motivation
- Difficulties
- Contributions
- Proposed Method
- Results
- Discussions
- References

Motivation

- Left atrial anatomy knowledge is clinically important due to its role in prognosis and risk stratification of several cardiovascular diseases.
- Functional assessment of the left atrium is often performed using cine MRI or echocardiography while both CT and MRI can be used for anatomical assessment.
- Most of the literature study focus on automated delineation on left ventricle only.
- Manual segmentation is time-consuming and tedious.

Difficulties

1. The wall of the left atrium is relatively thinner compared to left ventricle



Copyright © Addison Wesley Longman, Inc.

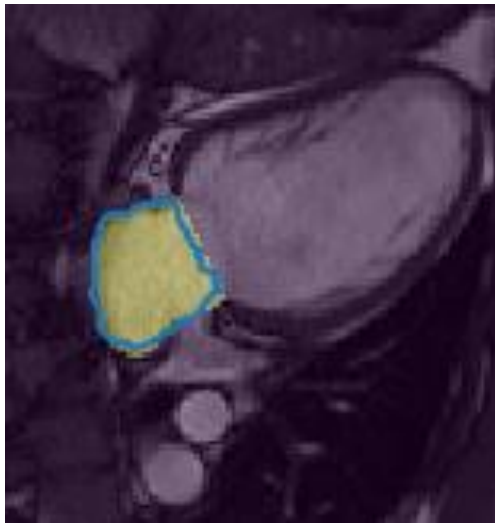
Difficulties

2. Boundaries are not clearly defined when the blood pool of the left atrium goes into pulmonary veins

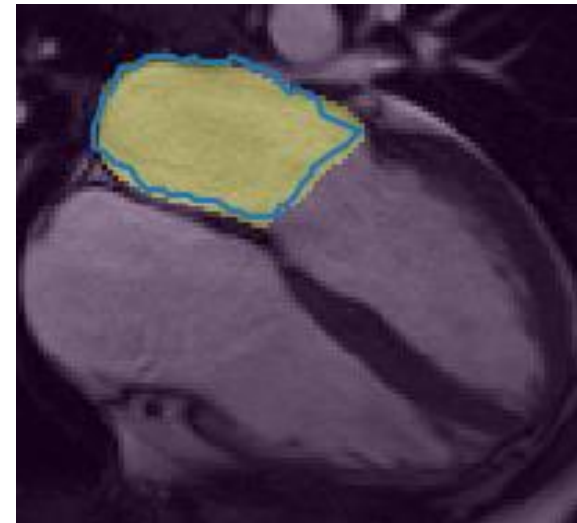


Difficulties

3. The shape variability of the left atrium is large between patients



Subject 1
3-chamber view

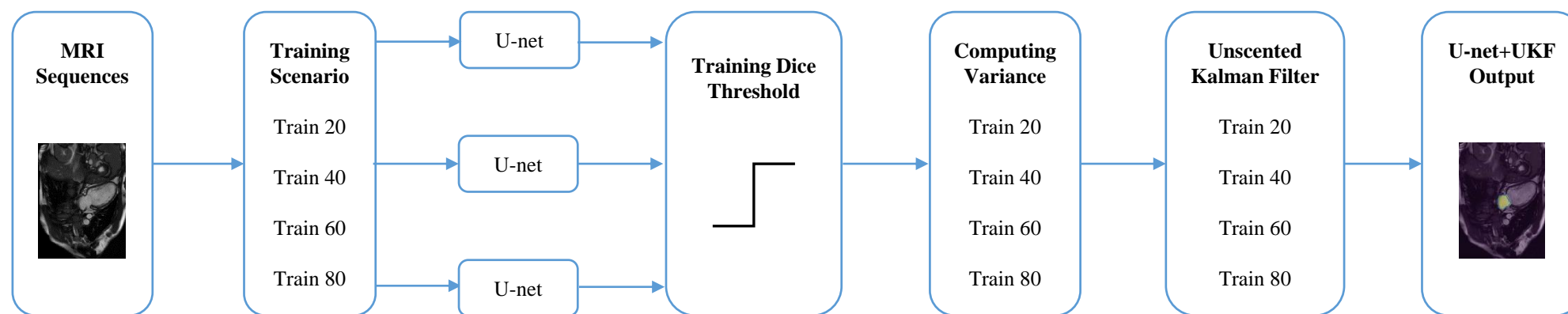


Subject 2
3-chamber view

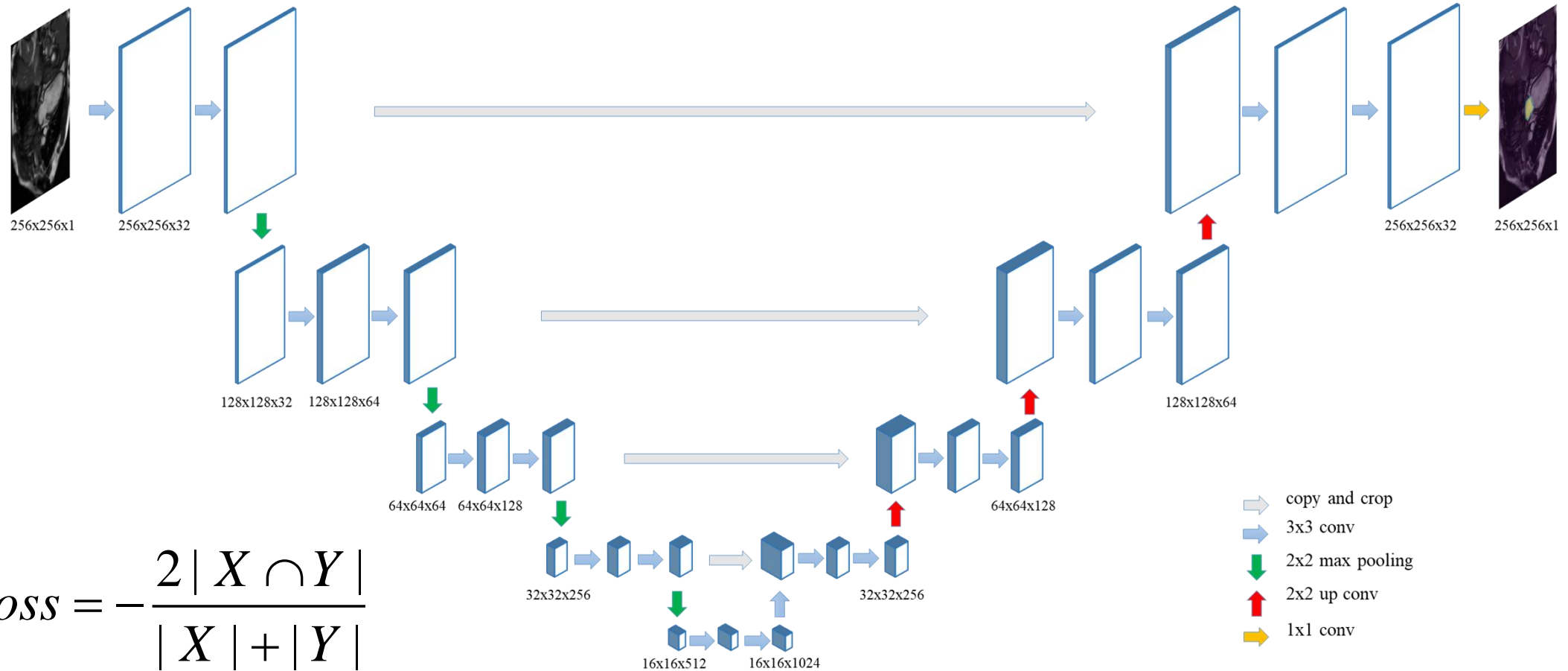
Contributions

1. A modified U-net [1] based deep convolutional neural network with dice loss is proposed for MR sequences.
2. Step activation function is utilized after training three separate models with 5-fold cross validation to reduce the impact of invalid training on prediction.
3. Unscented Kalman filter is utilized for image with high variance after calculating the intensity of each image predicted by U-net.
4. Time-varying angular frequency is implemented in UKF model to better delineate cardiac motion which is usually considered as a simple harmonic motion.
5. The study empirically assesses the impact of the amount of training samples on the network by comparing the performance of methods trained with data sets from 20, 40, 60, 80 patients.

Our Method



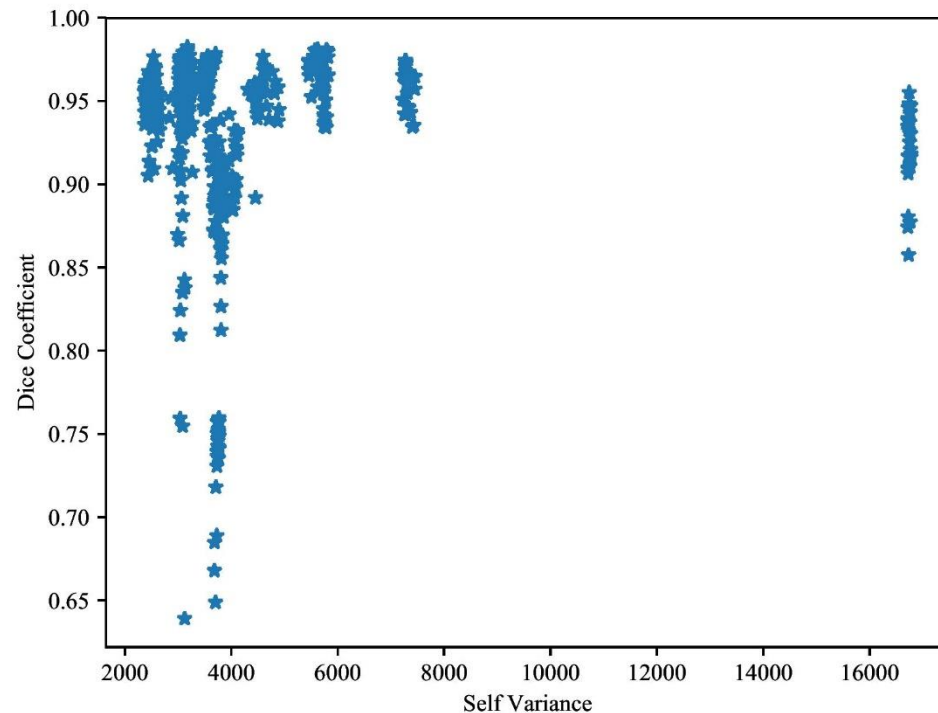
Modified U-net Architecture



$$loss = -\frac{2|X \cap Y|}{|X| + |Y|}$$

Variance Computation

- We notice that images with high variance cannot be predicted properly by our modified U-net structure. Thus, we set a step activation function to select those images that need to be processed, where a is the self variance value for each image and y is the binary label indicating the selection decision.



$$y = \begin{cases} 1 & a > 3000 \\ 0 & 0 \leq a \leq 3000 \end{cases}$$

Unscented Kalman Filter

- **State variable selection:** planar mean position, velocity, current position and time-varying angular velocity

$$S_k = [\bar{x}_k \ x_k \ \dot{x}_k \ \bar{y}_k \ y_k \ \dot{y}_k \ \omega_k]$$

where k indicates the number of frames between heart beat. In our case $k=25$ or 30 .

- **Discrete-time dynamic model:**

$$S_{k+1} = f_k(S_k) + v_k$$

where $f_k(S_k)$ is the prediction equation and v_k denotes a Gaussian process noise sequence.

Unscented Kalman Filter

$$f_k(S_k) = \begin{bmatrix} F_k & 0_{3 \times 3} & 0_{3 \times 1} \\ 0_{3 \times 3} & F_k & 0_{3 \times 1} \\ 0_{3 \times 3} & 0_{3 \times 3} & 1 \end{bmatrix} \quad F_k = \begin{bmatrix} 1 & 0 & 0 \\ 1 - \cos(\omega_k \Delta T) & \cos(\omega_k \Delta T) & \frac{1}{\omega_k} \cos(\omega_k \Delta T) \\ \omega_k \sin(\omega_k \Delta T) & -\omega_k \sin(\omega_k \Delta T) & \cos(\omega_k \Delta T) \end{bmatrix}$$

where ω_k denotes the time-varying angular frequency and ΔT is the time interval in a cardiac cycle

$$\omega_k = \frac{2\pi \times HeartRate}{60} \quad \Delta T = \frac{60}{HeartRate \times k}$$

$$v_k = \begin{bmatrix} Q_k & 0_{3 \times 3} & 0_{3 \times 1} \\ 0_{3 \times 3} & Q_k & 0_{3 \times 1} \\ 0_{3 \times 3} & 0_{3 \times 3} & 1 \end{bmatrix}$$

Unscented Kalman Filter

where Q_k denotes the covariance of process noise [3] given by:

$$q_{11} = q_1^2 \Delta T \quad q_{12} = q_{21} = \frac{q_1^2 (\omega_k \Delta T - \sin(\omega_k \Delta T))}{\omega_k} \quad q_{13} = q_{31} = q_1^2 (1 - \cos(\omega_k \Delta T))$$

$$q_{22} = \frac{q_1^2 \omega_k^2 (3\omega_k \Delta T - 4\sin(\omega_k \Delta T) + \cos(\omega_k \Delta T)) + q_2^2 \sin^2(\omega_k \Delta T)}{\omega_k}$$

$$q_{23} = q_{32} = \frac{q_1^2 \omega_k^2 (1 - 2\cos(\omega_k \Delta T) + \cos^2(\omega_k \Delta T)) + q_2^2 \sin^2(\omega_k \Delta T)}{2\omega_k^2}$$

$$q_{33} = -\frac{q_1^2 \cos(\omega_k \Delta T) \sin(\omega_k \Delta T) - q_2^2 (\cos(\omega_k \Delta T) \sin(\omega_k \Delta T) - \omega_k \Delta T)}{2\omega_k}$$

Unscented Kalman Filter

- **Update Equation:** measurement equation, aka update equation, is given by $z_k = H_k S_k + \eta_k$ in order to extract variables for UKF output. The measurement matrix is given as follows to extract position in x and y coordinate. η_k Denotes a zero mean Gaussian noise where $r=1e-2$.

$$H_k = \begin{bmatrix} 0 & 1 & 0 & 0 & 0 & 0 & 0 \\ 0 & 0 & 0 & 0 & 1 & 0 & 0 \end{bmatrix}$$

$$\eta_k = \begin{bmatrix} r & 0 \\ 0 & r \end{bmatrix}$$

Unscented Kalman Filter

- **Initialization:** A two-point difference method is implemented to initialize the unscented Kalman filter. The initial value in x coordinate in the state vector is given by:

$$\hat{x}_1 = z_{1,i} \quad \hat{\dot{x}}_1 = \frac{z_{2,j} - z_{1,j}}{\Delta T} \quad \hat{\ddot{x}}_1 = \frac{1}{k} \sum_{j=1}^k z_{j,i}$$

the corresponding initial covariance is given by:

$$P_1 = \begin{bmatrix} \phi_1 & 0_{3 \times 3} & 0_{3 \times 1} \\ 0_{3 \times 3} & \phi_1 & 0_{3 \times 1} \\ 0_{3 \times 3} & 0_{3 \times 3} & 1 \end{bmatrix}$$

$$\phi_1 = \begin{bmatrix} r & \frac{r}{k} & \frac{r}{k\Delta T} \\ \frac{r}{k} & r & \frac{r}{\Delta T} \\ \frac{r}{k\Delta T} & \frac{r}{k\Delta T} & \frac{2r}{\Delta T^2} \end{bmatrix}$$

Results

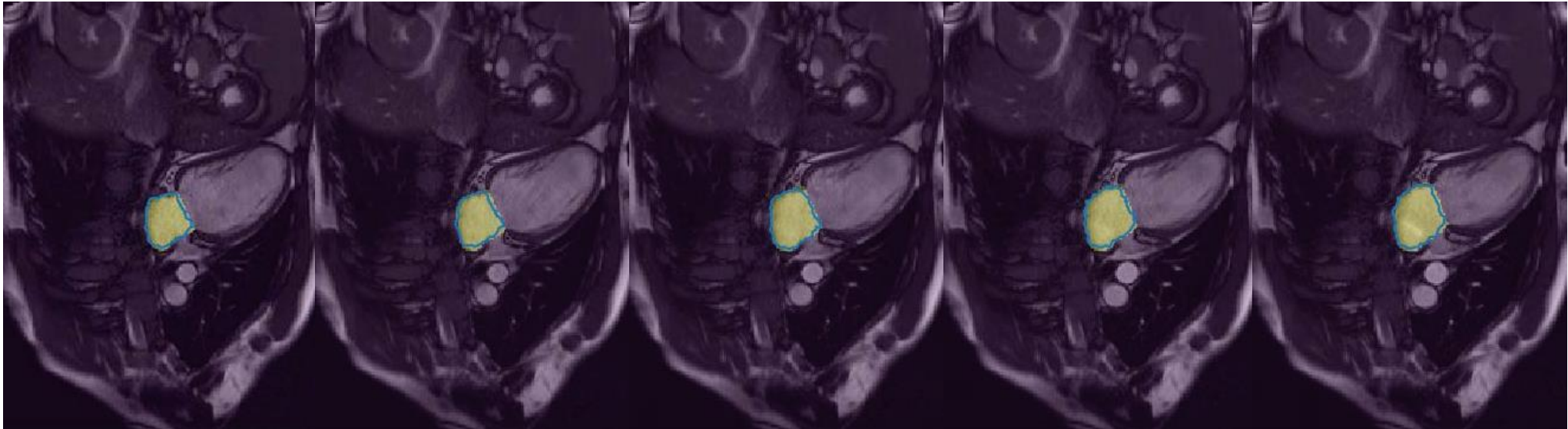
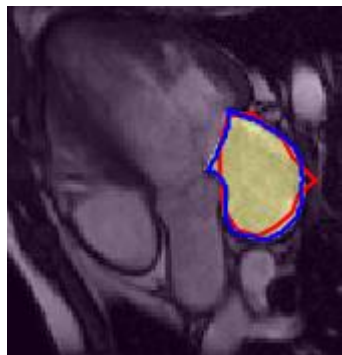
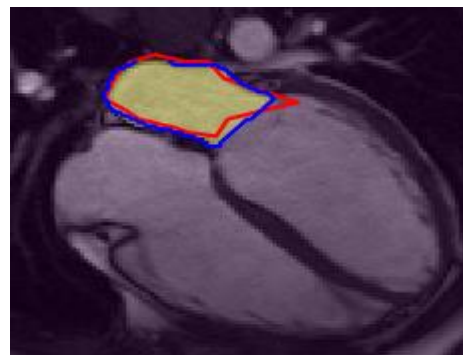


Figure: U-net+UKF prediction results in MRI sequences. For each image, the yellow area is the desired label and blue contour is the prediction results

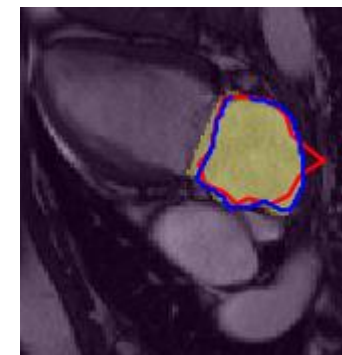
Results



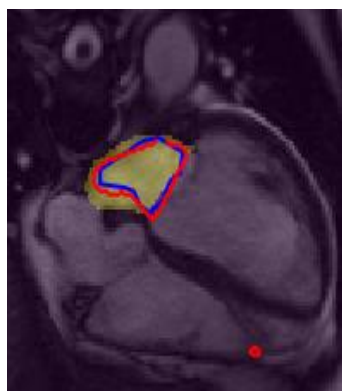
Subject 1 2-chamber view



Subject 1 3-chamber view



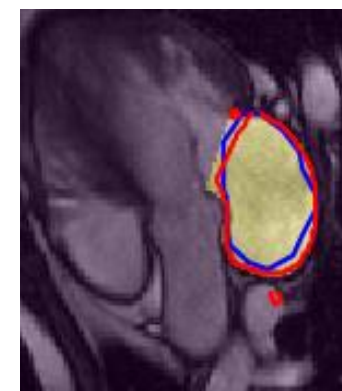
Subject 1 4-chamber view



Subject 2 2-chamber view



Subject 2 3-chamber view



Subject 2 4-chamber view

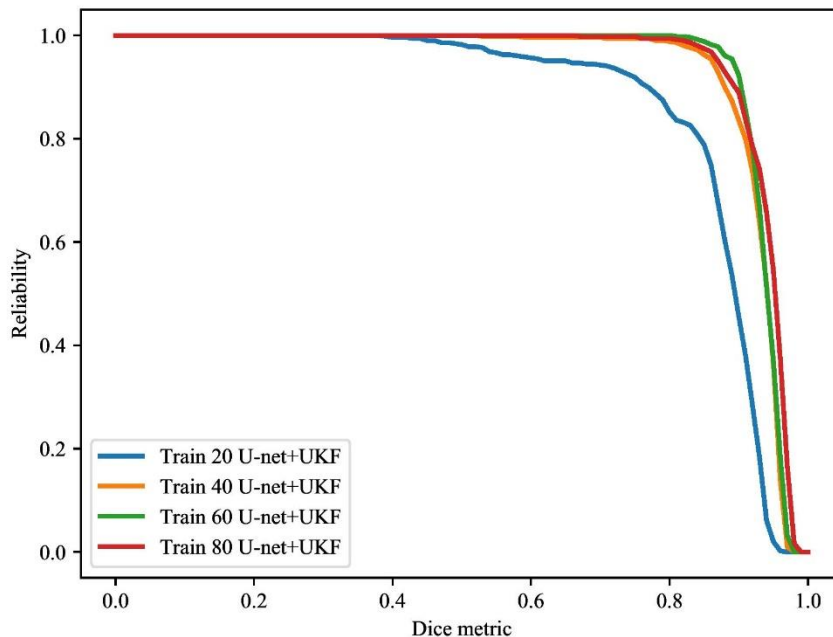
Results

Method	Dice Coefficient		Hausdorff Distance		Root Mean Square Error	
	U-net	U-net+UKF	U-net	U-net+UKF	U-net	U-net+UKF
Train 20	0.825±0.135	0.868±0.097	12.188±8.538	10.228±7.727	10.843±5.870	8.495±5.307
Train 40	0.918±0.076	0.929±0.042	8.603±6.845	7.652±6.187	8.575±5.255	6.944±4.187
Train 60	0.937±0.026	0.937±0.027	6.657±3.512	5.956±2.924	6.638±2.753	5.408±2.330
Train 80	0.933±0.058	0.941±0.037	7.022±4.319	6.020±3.308	6.191±3.474	5.373±3.192

Table: Validation results for patients. Dice coefficient illustrates the overlap accuracy between prediction masks with desired labels. Hausdorff distance reports the distance of largest pixel deviation from prediction contours with desired ones. RMSE demonstrates the standard deviation between prediction masks with label images.

Reliability Analysis

- In order to evaluate the impact of training samples on prediction performance, we calculate dice metric versus reliability [2].
- The ideal curve lies in the right upper corner. From the figure, we can find that there is a significant improvement from Train 20 to 60 while the improvement is minor from Train 60 to 80.



$$S(t) = P(\{T > t\}) = \int_t^{\infty} f(u)du = 1 - F(t)$$

Discussions

- Test evaluation of 505 images obtained from additional 20 patients shows that the proposed method yielded a promising accuracy of 94.1% for dice coefficient, 6.0 mm for Hausdorff distance, 5.4 mm for root mean square error.
- The quantitative assessment showed that the proposed method performs better than traditional U-net.

References

- [1] Ronneberger, O., Fischer, P., & Brox, T. (2015, October). U-net: Convolutional networks for biomedical image segmentation. In International Conference on Medical image computing and computer-assisted intervention (pp. 234-241). Springer, Cham.
- [2] Ayed, I. B., Punithakumar, K., Li, S., Islam, A., & Chong, J. (2009, September). Left ventricle segmentation via graph cut distribution matching. In International Conference on Medical Image Computing and Computer-Assisted Intervention (pp. 901-909). Springer, Berlin, Heidelberg.
- [3] Afshin, M., Ayed, I. B., Punithakumar, K., Law, M. W., Islam, A., Goela, A., ... & Li, S. (2014). Regional assessment of cardiac left ventricular myocardial function via mri statistical features. IEEE Trans. Med. Imaging, 33(2), 481-494.